Chinese Chemical Letters 36 (2025) 110508

Contents lists available at ScienceDirect

Chinese Chemical Letters

journal homepage: www.elsevier.com/locate/cclet

Transdermal delivery of amphotericin B using deep eutectic solvents for antifungal therapy

Bing Xie[a,1], Qi Jiang[a,1], Fang Zhu[b,1], Yaoyao Lai[a], Yueming Zhao[b,*], Wei He[a,c,*], Pei Yang[d,*]

[a] School of Pharmacy, China Pharmaceutical University, Nanjing 211198, China
[b] Department of Respiratory and Critical Medicine, Nanjing First Hospital, Nanjing Medical University, Nanjing 210000, China
[c] Key Laboratory of Modern Preparation of TCM, Ministry of Education, Jiangxi University of Chinese Medicine, Nanchang 330004, China
[d] School of Science, China Pharmaceutical University, Nanjing 211198, China

ARTICLE INFO

Article history:
Received 2 August 2024
Revised 23 September 2024
Accepted 25 September 2024
Available online 26 September 2024

Keywords:
Amphotericin B
Deep eutectic solvents
Transdermal delivery
Candida albicans
Fungal infections

ABSTRACT

Candida albicans is one of the most common pathogens causing invasive fungal infections, with a mortality rate of up to 20%–50%. Amphotericin B (AmB), a biopharmaceutics classification system (BCS) IV drug, significantly inhibits *Candida albicans*. AmB is primarily administered *via* oral and intravenous infusion, but severe infusion adverse effects, nephrotoxicity, and potential hepatotoxicity limit its clinical application. Deep eutectic solvents (DESs), with excellent solubilization ability and skin permeability, are attractive for transdermal delivery. Herein, we used DESs to deliver AmB for antifungal therapy transdermally. We first prepared and characterized DESs with different stoichiometric ratios of choline (Ch) and geranate (Ge). DESs increased the solubility of AmB by a thousand-fold. *In vitro* and *in vivo*, skin permeation studies indicated that $DES_{1:2}$ (Ch and Ge in 1:2 ratio) had the most outstanding penetration and delivered fluorescence dye to the dermis layer. Then, $DES_{1:2}$-AmB was prepared and *in vitro* antifungal tests demonstrated that $DES_{1:2}$-AmB had superior antifungal effects compared to AmB and $DES_{1:2}$. Furthermore, $DES_{1:2}$-AmB was skin-irritating and biocompatible. In conclusion, DES=AmB provides a new and effective therapeutic solution for fungal infections.

About 6.5 million people worldwide suffer from invasive fungal infections each year, of which about 2.5 million die, posing a severe threat to human health [1]. Invasive fungal infections occur in the subcutaneous tissues and internal organs. *Candida*, especially *Candida albicans*, is one of the most common pathogens causing invasive fungal infections [2]. According to the list of fungal priority pathogens issued by the World Health Organization, *Candida albicans* belongs to the critical priority group, and its mortality rate of invasive infections is up to 20%–50% [3,4].

Amphotericin B (AmB) is a polyene antifungal antibiotic from the biopharmaceutics classification system (BCS) IV drug, exerting antifungal effects by disrupting the permeability of cell membranes and forming extramembranous aggregates [5]. Due to its broad-spectrum antifungal activity and low resistance, AmB is the gold standard drug for invasive fungal infections [6,7]. AmB is administered *via* oral and intravenous infusion, however, severe infusion adverse effects, nephrotoxicity, hemolysis, and poor oral absorption limit its clinical application [8,9]. For instance, AmBisome®, an approved liposomal formulation, can significantly reduce toxicity but suffers from high treatment costs and potential hepatotoxicity [10–12]. Therefore, developing a safe and low-cost strategy for the efficient delivery of AmB is urgent.

Transdermal delivery provides a non-invasive, highly compliant, and safe treatment option [13–15]. However, the stratum corneum (SC) comprises keratinocytes and intercellular lipids; only drugs with specific chemical properties can pass through it [16–18]. Deep eutectic solvents (DESs) are liquid mixtures that are primarily formed by hydrogen bonding between hydrogen bond acceptors and donors [19,20], also referred to as ionic liquids, as the two have a molar ratio of 1:1 [21,22]. DESs significantly increase the solubility and enhance the skin permeability of insoluble drugs, and have been widely used in the transdermal delivery of insoluble drugs, biomolecules, and rigid particles [23–26]. In particular, choline (Ch) and geranate (Ge)-based DESs exhibit superior biocompatibility and biodegradability and are attractive options for transdermal delivery [27].

In this study, we prepared Ch-Ge-based DESs-AmB to treat fungal infections *via* transdermal administration. We first prepared and characterized various DESs with different Ch-Ge stoichiometric

* Corresponding authors.
E-mail addresses: sabrina-zym@163.com (Y. Zhao), weihe@cpu.edu.cn (W. He), yangpei@cpu.edu.cn (P. Yang).
[1] These authors contributed equally to this work.

https://doi.org/10.1016/j.cclet.2024.110508
1001-8417/

ratios. DESs significantly improved AmB's solubility and skin permeability. More significantly, DESs-AmB exhibited excellent anti-*Candida albicans* activity without skin irritation. Therefore, DES-AmB is a promising strategy for the transdermal treatment of fungal infections.

First, DESs with different Ch-Ge stoichiometric ratios (4:1, 2:1, 1.5:1, 1:1, 1:2, and 1:4 ratios) were prepared by salt metathesis reaction, expressed as $DES_{4:1}$, $DES_{2:1}$, $DES_{1.5:1}$, $DES_{1:1}$, $DES_{1:2}$, and $DES_{1:4}$, respectively. DESs were transparent and clear liquids (Fig. S1 in Supporting information). Then, we characterized the DESs using proton nuclear magnetic resonance (^{1}H NMR) and Fourier-transform infrared spectroscopy (FTIR) (Fig. S2 in Supporting information). In the ^{1}H NMR spectroscopy, an upfield shift of H in the Ge-related fragment indicated the disruption of the original intermolecular hydrogen bonding and the formation of new hydrogen bonding in DESs. In the FTIR spectra, the absorption peaks of O–H and C=O in choline bicarbonate appeared at 3389.9 and 1624.1 cm^{-1}, respectively. The absorption peaks of O–H and C=O in Ge appeared at 2969.6 and 1691.8 cm^{-1}, respectively. The shifts of O–H and C=O absorption bands in DESs changed with the molar ratio of Ch and Ge. The O–H and C=O peaks in DESs shifted at 2967.4–3418.5 cm^{-1} and 1621.4–1692.1 cm^{-1}. The results confirmed the formation of DESs.

Next, we studied the DES's ability to solubilize AmB and transdermally deliver the payloads. DESs demonstrated significant solubility enhancement of the drug. The AmB solubility in DESs was 110–5585 times higher than in water (Fig. 1A and Table S1 in Supporting information). Then, we tested the skin penetration of DESs-1,1′-dioctadecyl-3,3,3′,3′-tetramethylindotricarbocyanine iodide (DiR) and -fluorescein isothiocyanate (FITC). The cumulative DiR-penetration amounts from DESs ($DES_{4:1}$, $DES_{2:1}$, $DES_{1.5:1}$, $DES_{1:1}$, $DES_{1:2}$, and $DES_{1:4}$) were 23.13 ± 0.40, 24.46 ± 0.32, 25.96 ± 1.34, 26.30 ± 2.50, 28.74 ± 1.05, and 26.93 ± 1.48 ng/cm^2, respectively (Fig. 1B). The results indicated that DESs improved the skin penetration of DiR compared to DiR solution, and $DES_{1:2}$ had the highest penetration ability. Furthermore, the penetration depth of DESs-FITC *in vitro* was observed using fluorescence microscope (Fig. 1C). DESs-FITC passed through the SC and diffused into the epidermis and dermis layers. Again, $DES_{1:2}$-FITC showed higher penetration than other DESs (Fig. 1D). This enhanced skin permeability may be attributed to DESs' lipid extraction [28]. Moreover, increasing Ch in DESs compromised the skin permeability due to high viscosity and high hydrophilicity [29]. As a result, the penetration elevated as the Ch-Ge stoichiometric ratio reduced from 4:1 to 1:2.

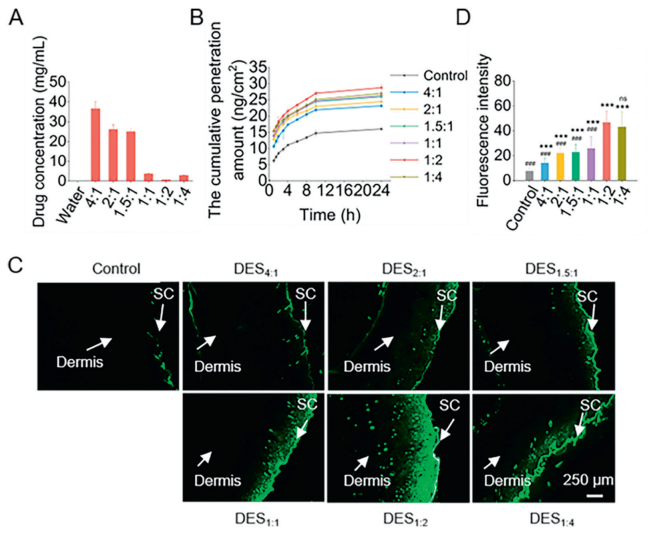

Fig. 1. Solubilization and permeation enhancement. (A) Equilibrium solubility of AmB in DESs with different stoichiometry. (B) The cumulative penetration amount of DESs-DiR *in vitro*. (C) *In vivo* DESs-FITC permeation into rat skin (SC, stratum corneum). Scale bar: 250 μm. (D) Semi-quantitative analysis of FITC fluorescence intensity (mean ± SD, $n = 20$). $^{***}P < 0.001$ *vs.* the control group; $^{###}P < 0.001$ *vs.* $DES_{1:2}$-FITC group. ns, no significance.

To characterize the drug-loading DES, we prepared DES-AmB (with 1 mg/mL AmB) by vortexing and sonication. DES-AmB exhibited a clarified and transparent appearance (Fig. S3 in Supporting information). To verify the interaction between AmB and DES, we performed the test of FTIR and ^{1}H NMR of $DES_{1:2}$-AmB. The ^{1}H NMR peaks at δ 6.41–5.99 and 1.23–0.91 ppm in AmB disappeared in $DES_{1:2}$-AmB, indicating the interactions between AmB and $DES_{1:2}$ (Fig. 2A). As shown in Fig. 2B, the O–H stretching vibration peak in AmB shifted from 3383.9 cm^{-1} to 3396.7 cm^{-1}. The C=O stretching vibration peak in AmB shifted from 1689.5 cm^{-1} to 1645.3 cm^{-1}, demonstrating the hydrogen bonding in $DES_{1:2}$-AmB.

DESs have self-assembling behavior in water and form colloidal systems, such as micelles or emulsions, due to the hydrophilic of Ch and hydrophobic tails of Ge [30–32]. In addition, the micellar structure can increase skin permeability through diffusion and fusion during transdermal drug delivery [33]. Here, we diluted DES-AmB to 30% (v/v) using water and measured the particle size (Fig. 2C and Table S2 in Supporting information). The formulation of 30% $DES_{1:2}$-AmB demonstrated the most minor diameter (14.08 ± 1.90 nm, PDI 0.282 ± 0.012). In contrast, other formulations of 30% DES-AmB displayed a significant increase in particle size and PDI, likely due to the compromising interaction between the drug and DESs and the ratios of Ch-Ge [29,34]. Transmission electron microscopy (TEM) examination displayed that the 30% $DES_{1:2}$-AmB nanocomplexes were sub-spherical (Fig. 2D). In the differential scanning calorimetry (DSC) spectra (Fig. 2E), AmB and $DES_{1:2}$ showed heat-absorption peaks at 205 and 241 °C, respectively. $DES_{1:2}$-AmB had a heat-absorption peak at 239 °C with a similar peak to $DES_{1:2}$, indicating that AmB was miscible with $DES_{1:2}$.

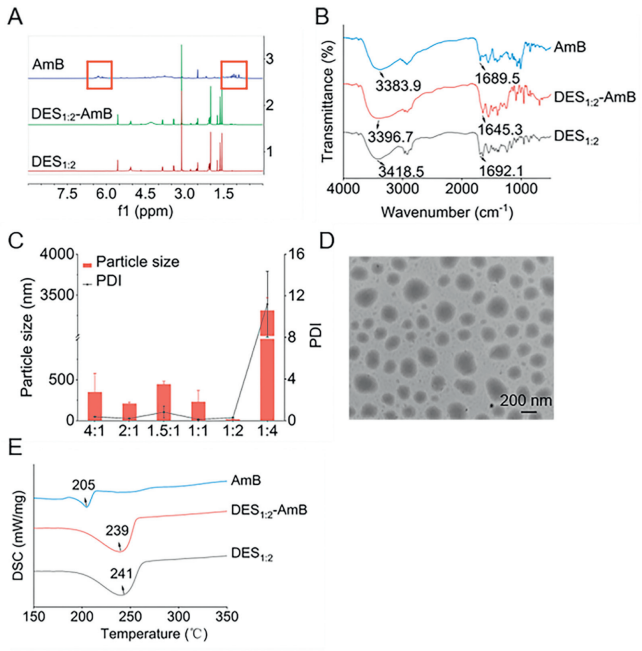

Fig. 2. Preparation and characterization of DESs-AmB. (A) ^{1}H NMR and (B) FTIR spectra of AmB, $DES_{1:2}$-AmB and $DES_{1:2}$. (C) Particle size and PDI of 30% DESs-AmB. (D) TEM image of 30% $DES_{1:2}$-AmB (scale bar: 200 nm). (E) DSC thermograms of AmB, $DES_{1:2}$-AmB and $DES_{1:2}$.

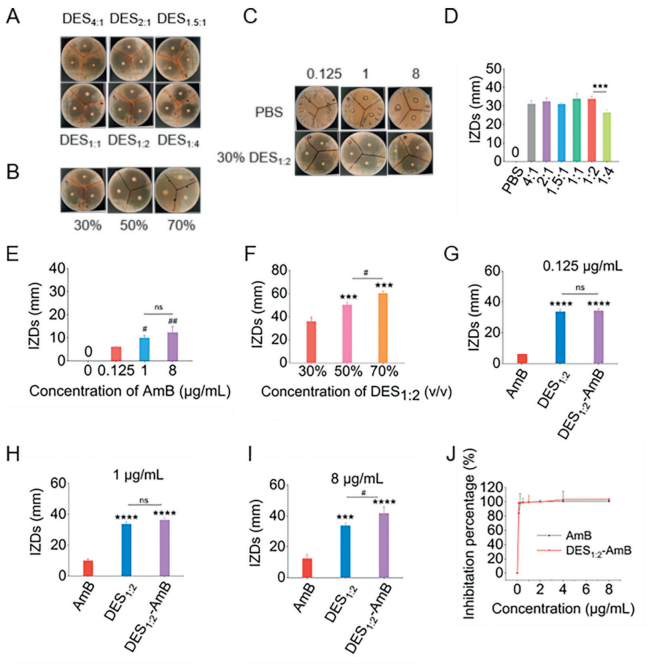

Fig. 3. Antifungal activity *in vitro*. (A) The inhibitory circle of DESs. (B) The inhibitory circle of $DES_{1:2}$ with different concentrations. (C) The inhibitory circle of AmB and $DES_{1:2}$-AmB. (D) The IDZs of DESs ($^{***}P < 0.001$). (E) The IDZs of AmB with different concentrations ($^{\#}P < 0.05$, $^{\#\#}P < 0.01$ *vs.* 0.125 μg/mL). (F) The IDZs of $DES_{1:2}$ with various concentrations ($^{***}P < 0.001$ *vs.* the 30% $DES_{1:2}$; $^{\#}P < 0.05$). (G-I) The IDZs of AmB, $DES_{1:2}$ and $DES_{1:2}$-AmB. The concentration of AmB was 0.125, 1, and 8 μg/mL ($^{***}P < 0.001$, $^{****}P < 0.0001$ *vs.* the AmB group; $^{\#}P < 0.05$). (J) The minimum inhibitory concentration of AmB and $DES_{1:2}$-AmB. Data are presented as mean ± SD, $n = 3$.

As shown in Fig. S4 (Supporting information), storage stability indicated that the AmB content in $DES_{1:2}$-AmB remained constant after one-month storage at 4 °C (Figs. S4A and B). However, long-term testing indicated that the drug content in 30% $DES_{1:2}$-AmB decreased significantly under similar storage conditions (Fig. S4C). AmB in 30% $DES_{1:2}$-AmB was almost completely degraded under high temperature, high humidity and intense light due to the sensitivity of AmB to water, light, and temperature (Figs. S4D–G). The results indicated that $DES_{1:2}$-AmB instead of 30% $DES_{1:2}$-AmB should be stored at low temperature and low humidity and protected from light. We also found that the drug stability was related to the Ch-Ge stoichiometric ratios in DES.

The antifungal effects of DESs and AmB were studied by measuring the inhibition zone diameters (IZDs) (Figs. 3A–C). DESs with different stoichiometric ratios significantly inhibited *Candida albicans*, and the antifungal effect of $DES_{1:2}$ was comparable to that of other DESs except for $DES_{1:4}$ (Fig. 3D). $DES_{1:2}$ and AmB enhanced antifungal activity in a dose-dependent manner (Figs. 3E and F). Considering the convenience and applicability, 30% $DES_{1:2}$-AmB with appropriate flowability was selected for the following study. When the concentration of AmB was 0.125, 1, and 8 μg/mL, the IZDs of $DES_{1:2}$-AmB were more significant than that of AmB (Figs. 3G–I). In particular, when the concentration of AmB was 8 μg/mL, the IZDs of $DES_{1:2}$-AmB were 1.2 and 3.4 times higher than those of $DES_{1:2}$ and AmB, respectively, and the significant difference indicated the synergistic antifungal effects between $DES_{1:2}$ and AmB (Fig. 3I).

The minimum inhibitory concentration (MIC_{90}) of AmB and $DES_{1:2}$-AmB was further performed to evaluate the antifungal ability. The MIC_{90} of AmB and $DES_{1:2}$-AmB were 0.25 and 0.125 μg/mL, respectively (Fig. 3J). The antifungal effect of $DES_{1:2}$-AmB may be attributed to several antifungal mechanisms. AmB binds to ergosterol on fungal cell membranes, creating micropores and killing the fungus [35]. Recent studies have shown that AmB extracts ergosterol and forms extramembranous aggregates to exert antifungal effects [36,37]. DESs may extract or fluidize microbial membrane lipids [38,39]. The results indicated that combining DESs and antifungal drugs could be an effective strategy against fungal infections.

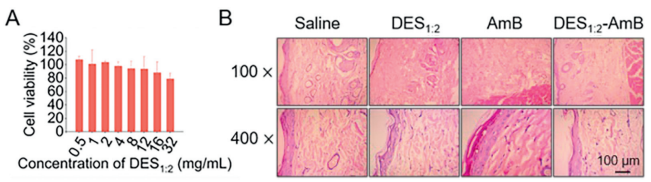

Fig. 4. Safety evaluation. (A) *In vitro* cytotoxicity of $DES_{1:2}$ (mean ± SD, $n = 6$). (B) Histopathological evaluation of rats' skin sections treated with saline, $DES_{1:2}$, AmB and $DES_{1:2}$-AmB (scale bar: 100 μm).

Finally, safety was assessed by studying the cytotoxicity and skin irritation. The viability of human immortalized epidermal (HaCaT) cells decreased with the increase of $DES_{1:2}$ concentration. When the concentration of $DES_{1:2}$ reached 16 mg/mL, the survival rate of HaCaT cells was still higher than 80%, indicating that $DES_{1:2}$ had a comprehensive safety range (Fig. 4A). In addition, histopathological analysis revealed that the treatment using $DES_{1:2}$-AmB showed a tight connection between the SC, epidermis layer, and dermis layer and allowed little inflammatory cell infiltration and necrosis compared to saline administration (Fig. 4B), indicating biocompatibility. All the animal experimental were performed according to the protocols approved by China Pharmaceutical University Institutional Animal Care and Use Committee (No. 202409016).

In summary, the Ch-Ge-based DESs could dramatically solubilize AmB and improve transdermal delivery. Notably, $DES_{1:2}$ possessed potent antifungal effects, and its combined application with AmB exhibited excellent inhibition of *Candida albicans* without significant skin irritation. $DES_{1:2}$-AmB is promising to treat dermatologic conditions caused by fungal infections and has the potential for clinical translation. In addition, due to simple composition and preparation, $DES_{1:2}$-AmB could be adapted to other antifungal and antibacterial drugs, reducing resistance and improving therapeutic efficacy.

Declaration of competing interest

The authors declare that they have no known competing financial interests or personal relationships that could have appeared to influence the work reported in this paper.

CRediT authorship contribution statement

Bing Xie: Writing – original draft, Methodology, Investigation. **Qi Jiang:** Methodology, Investigation, Formal analysis, Data curation. **Yaoyao Lai:** Methodology, Formal analysis, Data curation. **Yueming Zhao:** Writing – review & editing, Validation, Supervision, Investigation, Data curation, Conceptualization. **Wei He:** Writing – review & editing, Supervision, Project administration, Funding acquisition, Formal analysis, Data curation, Conceptualization. **Pei Yang:** Writing – review & editing, Supervision, Methodology, Investigation, Formal analysis, Data curation, Conceptualization.

Acknowledgments

This study was supported by the National Natural Science Foundation of China (Nos. 81872823, 82073782, and 82241002) and the Key R&D Plan of Ganjiang New District of Jiangxi (No. 2023010).

Supplementary materials

Supplementary material associated with this article can be found, in the online version, at doi:10.1016/j.cclet.2024.110508.

References

[1] D.W. Denning, Lancet Infect. Dis. 24 (2024) e428–e438.
[2] C. Lass-Flörl, S.S. Kanj, N.P. Govender, et al., Nat. Rev. Dis. Primers 10 (2024) 20.
[3] P. Koehler, M. Stecher, O.A. Cornely, et al., Clin. Microbiol. Infect. 25 (2019) 1200–1212.
[4] J.T. Loh, K.P. Lam, Adv. Drug Deliv. Rev. 196 (2023) 114775.
[5] R. Fernández García, J.C. Muñoz García, M. Wallace, et al., J. Control. Release 341 (2022) 716–732.
[6] X. Wang, I.S. Mohammad, L.F. Fan, et al., Acta Pharm. Sin. B 11 (2021) 2585–2604.
[7] J.R. Perfect, Nat. Rev. Drug Discov. 16 (2017) 603–616.
[8] Y. Lee, E. Puumala, N. Robbins, L.E. Cowen, Chem. Rev. 121 (2021) 3390–3411.
[9] K. Thapa Magar, G.F. Boafo, X.T. Li, Z.J. Chen, W. He, Chin. Chem. Lett. 33 (2022) 587–596.
[10] R.J. Hamill, Drugs 73 (2013) 919–934.
[11] N.R. Stone, T. Bicanic, R. Salim, W. Hope, Drugs 76 (2016) 485–500.
[12] Q.Y. Liu, J.H. Zou, Z.J. Chen, W. He, W. Wu, Acta Pharm. Sin. B 13 (2023) 4391–4416.
[13] V. Phatale, K.K. Vaiphei, S. Jha, et al., J. Control. Release 351 (2022) 361–380.
[14] M. Qindeel, M.H. Ullah, D. Fakhar Ud, N. Ahmed, A.U. Rehman, J. Control. Release 327 (2020) 595–615.
[15] Y. Zhang, C.L. Liu, J.Q. Wang, et al., Chin. Chem. Lett. 34 (2023) 107631.
[16] D. Ramadon, M.T.C. McCrudden, A.J. Courtenay, R.F. Donnelly, Drug Deliv. Transl. Res. 12 (2022) 758–791.
[17] Y.Z. Chen, J.J. Zhu, J.S. Ding, W.H. Zhou, Chin. Chem. Lett. 35 (2024) 108706.
[18] T.T. Zhang, X. Luo, K.M. Xu, W.Y. Zhong, Adv. Drug Deliv. Rev. 203 (2023) 115139.
[19] M.H. Zainal-Abidin, M. Hayyan, G.C. Ngoh, W.F. Wong, C.Y. Looi, J. Control. Release 316 (2019) 168–195.
[20] Y.W. Liu, Y.J. Wu, J.M. Liu, et al., Int. J. Pharm. 622 (2022) 121811.
[21] A.A. Quintana, A.M. Sztapka, V.C. Santos Ebinuma, C. Agatemor, Angew. Chem. Int. Ed. 61 (2022) e202205609.
[22] A.M. Curreri, J. Kim, M. Dunne, et al., Adv. Sci. 10 (2023) e2205389.
[23] V. Dharamdasani, A. Mandal, Q.M. Qi, et al., J. Control. Release 323 (2020) 475–482.
[24] Z.Y. Zhao, M.J. Li, L.Y. Zheng, et al., J. Control. Release 343 (2022) 43–56.
[25] M.J. Li, H. Cui, Y.B. Cao, et al., J. Control. Release 354 (2023) 664–679.
[26] J.X. Zhu, Y.F. Wei, J.J. Zhang, et al., J. Colloid Interface Sci. 645 (2023) 813–822.
[27] X.D. Li, N.N. Ma, L.J. Zhang, G.X. Ling, P. Zhang, Int. J. Pharm. 612 (2022) 121366.
[28] Q.M. Qi, S. Mitragotri, J. Control. Release 311-312 (2019) 162–169.
[29] E.E.L. Tanner, K.N. Ibsen, S. Mitragotri, J. Control. Release 286 (2018) 137–144.
[30] Y.J. Shi, Z.M. Zhao, Y.S. Gao, et al., J. Control. Release 322 (2020) 602–609.
[31] Y.J. Shi, Z.M. Zhao, K. Peng, et al., Adv. Healthc. Mater. 10 (2021) e2001455.
[32] M.N. Huda, I.G. Deaguero, E.A. Borrego, et al., J. Control. Release 349 (2022) 783–795.
[33] B. Li, S.W. Jiao, S.Q. Guo, et al., J. Nanobiotechnol. 22 (2024) 272.
[34] Y.M. Demirlenk, H. Albadawi, Z. Zhang, et al., Sci. Transl. Med. 16 (2024) eadn7982.
[35] Y. Liu, Y. Han, T. Fang, et al., J. Control. Release 324 (2020) 657–668.
[36] T.M. Anderson, M.C. Clay, A.G. Cioffi, et al., Nat. Chem. Biol. 10 (2014) 400–406.
[37] A. Lewandowska, C.P. Soutar, A.I. Greenwood, et al., Nat. Struct. Mol. Biol. 28 (2021) 972–981.
[38] M. Zakrewsky, A. Banerjee, S. Apte, et al., Adv. Healthc. Mater. 5 (2016) 1282–1289.
[39] K.N. Ibsen, H. Ma, A. Banerjee, et al., ACS Biomater. Sci. Eng. 4 (2018) 2370–2379.